



Article

Mosaic Technology in the Armenian Chapel Birds Mosaic, Jerusalem: Characterizing the Polychrome Hidden *Sinopia*

Yotam Asscher ^{1,2,*}, Giulia Ricci ³ , Michela Reato ³, Ilana Peters ^{2,4}, Abraham Leviant ¹, Jacques Neguer ², Mark Avrahami ² and Gilberto Artioli ³ 

¹ Department of Culture Heritage, School of Archaeology and Maritime Cultures, University of Haifa, Haifa 3498838, Israel

² Artifacts Treatment and Conservation Department, Israel Antiquities Authority, Jerusalem 9100402, Israel

³ Department of Geosciences and CIRCe Centre, University of Padua, 35131 Padova, Italy

⁴ Department of Archaeology of the Biblical Period, Institute of Archaeology, Hebrew University of Jerusalem, Jerusalem 9190501, Israel

* Correspondence: yasscher@univ.haifa.ac.il

Abstract: Since the Hellenistic period, preparatory drawings known as *sinopiae* were employed as guidelines for mosaicists in creating mosaics. The *sinopiae* served as the basis for style and content, facilitating the placement of colored tesserae in the supporting mortar. The technology of the mosaic and pigments used reflect the capacity of the mosaic workshop and its master. This work explores a polychrome *sinopia* that was found under a Byzantine mosaic of an Armenian Chapel in Jerusalem, by a multi-analytical characterization of mineralogical and chemical properties. The composition of the pigments in the black and red areas of the *sinopia* include carbon black and red ochre, respectively, utilized in the fresco technique. Since colored tesserae are placed in wet mortar, it can be deduced that mosaicists worked together with painters during the executionary steps. This has corresponding implications for historical and artistic specializations at mosaic workshops, with deeper understanding of mosaic production processes. This research also highlights the importance of studying *sinopiae* under floor mosaics, which is a source of information on the pigments, paintings techniques, and the people who executed the work, all embedded in mortar which is well protected below the stone tesserae.

Keywords: *sinopia*; Byzantine; fresco; mosaics; pigments; XRD; XRF; SEM-EDS; Raman; FORS; FTIR



Citation: Asscher, Y.; Ricci, G.; Reato, M.; Peters, I.; Leviant, A.; Neguer, J.; Avrahami, M.; Artioli, G. Mosaic Technology in the Armenian Chapel Birds Mosaic, Jerusalem: Characterizing the Polychrome Hidden *Sinopia*. *Heritage* **2024**, *7*, 5462–5475. <https://doi.org/10.3390/heritage7100258>

Academic Editor: Francesco Soldovieri

Received: 26 June 2024

Revised: 11 September 2024

Accepted: 25 September 2024

Published: 30 September 2024



Copyright: © 2024 by the authors. Licensee MDPI, Basel, Switzerland. This article is an open access article distributed under the terms and conditions of the Creative Commons Attribution (CC BY) license (<https://creativecommons.org/licenses/by/4.0/>).

1. Introduction

In ancient times, occasionally a preparatory drawing of geometric or illustrative design, including incisions and pigments, would be used as a guideline for the mosaicist when inserting colored tesserae [1,2]. These guidelines, known as *sinopiae*, were used by the master mosaicist to determine the style and content of the mosaic, while the artisans completed the work by placing the colored stones [3]. The origin of the word “*sinopia*” refers to the red ochre that came from Sinop, Turkey (Şerifaki); however, *sinopiae* can vary between monochrome of red ochre or carbon black, or polychrome with a larger palette [4]. *Sinopiae* were used mainly in wall and floor mosaics in the Hellenistic and Roman periods, whereas during the Middle Ages they were also found under frescoes and wall paintings [5–7]. This technique continued to be utilized until the 16th century AD, whereupon it was substituted by other methods such as graffito and pounce [8]. The most vibrant and longest-lasting plaster paintings are based on the fresco technique, due to the penetration of the pigment within the wet lime [9].

The *sinopia* is a part of the complex structure that supports the stone tesserae, described historically by Vitruvius in the 1st century BC [10]. The structure includes levelling the bedrock with a thick preparatory layer of gravel and sand that acts as a solid base which levels the bedrock (statumen). The first layer of mortar with large pebbles or stones (rudus)

is placed above the statumen (levelled soil and gravel), and finally a fine upper layer of mortar (sovrannucleus) is laid above. The rudus acts as a gradient between the statumen and the sovrannucleus. This structure includes information on the mosaic-making process. Characterizing the pigments in the *sinopia* and the stone tesserae provides important insight on the mosaic workshop skills and expertise. The workshop should have been involved in procuring the raw materials, services, and specialists including lime manufacturers and painters [11]. The nature and quality of the materials allow differentiating between the workshops based on their access to precious raw materials, such as stones and pigments from foreign locations, which influences the understanding of ancient trade networks [12,13].

In the southern Levant, *sinopiae* have been noted under several Byzantine mosaics, such as those in Lod, Hura, 'Aluma, Horbat Fatot, and the Armenian quarter in Jerusalem [14]. A late Roman mosaic from a villa in Lod, dated to circa 300 AD, showed a polychrome *sinopia* including red and yellow ochre, green earth, carbon black, and cinnabar, all applied using the fresco technique [15,16]. The *sinopia* in this study was also polychrome. It was found in a Byzantine funerary chapel beneath the mosaic known as the "Birds Mosaic" or the "Armenian Mosaic" which was initially excavated over a century ago [17,18]. The date of the mosaic is based on an inscription found in the mosaic that shows stylistic criteria associated with the sixth century CE [19], in addition to a paleography study which suggests a date within the sixth–seventh centuries CE [20].

In 2019, the Birds Mosaic was moved to a better-equipped museum within the Armenian Quarter of the Old City of Jerusalem, as it was undergoing rapid deterioration due to the relative humidity in the chapel. During this time, a burial crypt located over two meters below the mosaic was rediscovered and radiocarbon dated between the fifth and the first half of the sixth century CE [14], leading to the designation of this complex as a funerary chapel. The discrepancy between the date of the inscription of the mosaic and the burial crypt suggests that the inscription and perhaps the entire mosaic is a later addition to the mortuary chapel. The chapel includes the apse in the east and was decorated with a mosaic with a chalice of fruits and flanked by birds. An Armenian inscription written in Erkat'agir script is located between the central panel and the apse, reading "For the memorial and salvation of all Armenians whose names the Lord knows" [20].

The Birds Mosaic floor measures 3.38×8.10 m and consists of a central panel and a small apse. The central panel of the mosaic has vine scrolls stemming from an amphora (Figure 1), which sits in an acanthus leaf and is flanked by two peacocks. These vine scrolls are inhabited by a variety of birds, that some interpretations suggest ducks, storks, a partridge, an eagle, and a parrot [18], while others do not include a parrot or ducks but rather a goose, an ibis, swallows, pheasants, doves, ostriches, multiple partridges, and a flamingo [21]. The vine scrolls form medallions around the birds, which are arranged symmetrically, similar to vine scrolls found at several contemporary sites such as Gaza, Ma'on, Shellal, Bet Guvrin, Khirbed 'Asida, Kyria Maria, and Jerash [19].

In the Birds Mosaics, the tessellatum is between a 13–15 mm-thick layer, including tesserae 10–13 mm and a fine lime bed mortar composed of lime and stone powder. The sovrannucleus is approximately a 15–20 mm-thick layer of very elastic lime mortar, composed of lime and crushed limestone aggregates of up to 2 mm. The rudus is made of a 40–50 mm-thick layer of lime mortar, composed of stone powder and crushed carbonate rock aggregates up to 4 mm, and the statumen showed one layer of stones, 50–60 mm in size, mixed with soil. The foundation of the mosaic lays on the bedrock in several places.

In this work, we study the production technique of the mosaic in the Armenian Chapel in Jerusalem, mainly by analyzing the painted *sinopia* and associated tesserae. We characterized black and red *sinopiae* and their associated black and red tesserae chemically and structurally. This research may hold significant importance due to its unique focus on the characterization of *sinopiae* in floor mosaics, as it is a subject that has received limited attention and is supported by a meagre number of archaeometric studies found in the literature [22].

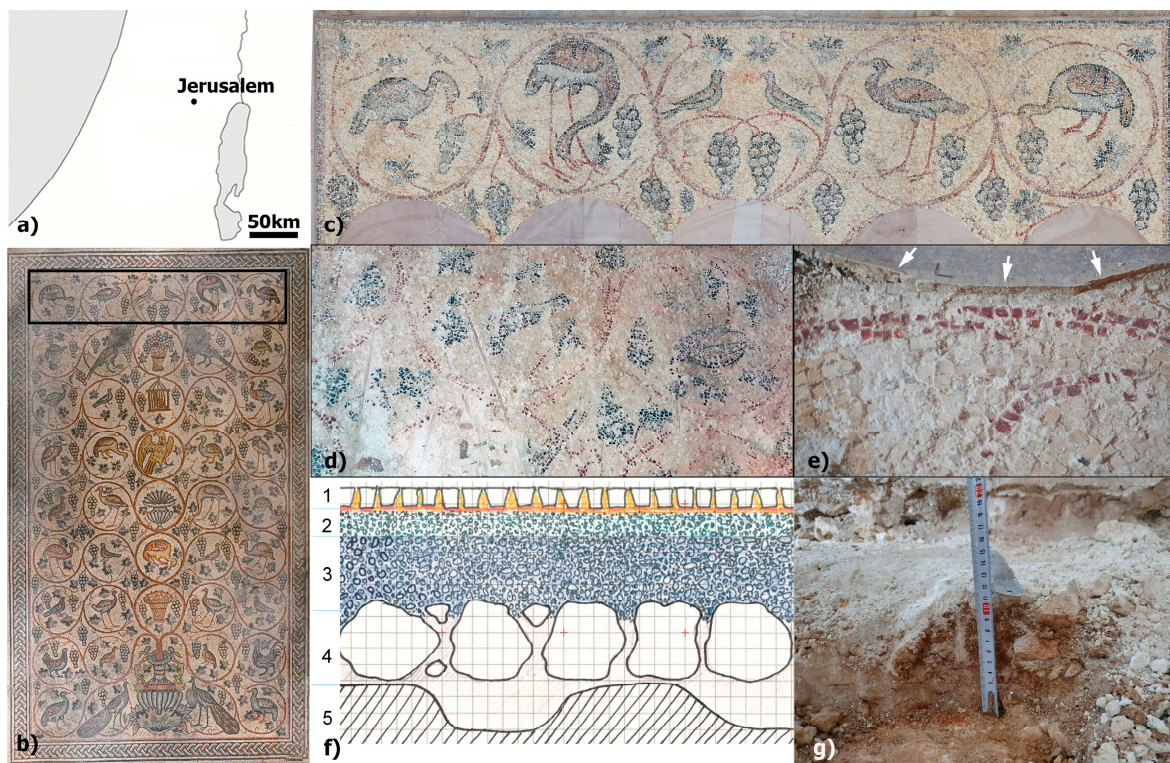


Figure 1. (a) A map of Israel with the location of Jerusalem. (b) The Birds Mosaic in Jerusalem showing vine scroll medallions surrounding a variety of animals. The studied *sinopia* was from the top part of the mosaic (marked with a black rectangle). (c) The area of the mosaic that was studied. (d) The painted mortar beneath the mosaic, showing the state of preservation of the polychrome *sinopia*. (e) A part of the red vine medallion of the *sinopia*. Note the overlying mosaic tesserae (marked with white arrows). (f) A schematic stratigraphy of the mosaic, showing (5) bedrock, (4) statumen, (3) rudus, (2) sovrannucleus, upon which the *sinopia* is painted on, and (1) the tesserae. Each square is 1 cm for scale. (g) The thickness of the statumen is approximately 100 mm.

2. Materials and Methods

Black and red tesserae and their associated painted mortars (*sinopia*) were analyzed by complementary techniques (Table 1). Samples are shown in Figure 2. Non-invasive characterization was performed prior to well-established techniques that require sampling; the significance of the non-invasive approach will be discussed in future work.

Petrographic analyses were performed by a transmitted-light optical microscope (TL-OM) on 30 μm -thin sections under parallel and crossed polars using a Nikon Eclipse ME600 microscope (Nikon Corp., Tokyo, Japan) equipped with a Canon EOS 600D Digital single-lens reflex camera (Canon Inc., Tokyo, Japan). The thin sections were microstructurally and microchemically characterized by FEI Quanta 200 environmental scanning electron microscopy (ESEM, Thermo Fisher Scientific/FEI, Hillsboro, OR, USA) equipped with EDS. EDS analysis was performed using Back Scattered Electrons (BSE) modality in single point and areas. Furthermore, elemental maps for chemical elements of interest, such as Al, Si, Ca, Mg, and Fe, were performed.

Mineralogical phase analyses were performed by XRD on the surface of the sample using a Malvern PANalytical X'Pert PRO diffractometer (Malvern Panalytical, Great Malvern, UK) in Bragg–Brentano geometry, Co–K α radiation, 40 kV, and 40 mA, equipped with a real-time multiple strip (RTMS) detector (X'Celerator by Malvern Panalytical). Data acquisition was performed by operating a continuous scan in the range of 3–85° 2 θ , with a virtual step scan of 0.02° 2 θ . Diffraction patterns were interpreted with X'Pert HighScore Plus 3.0 software by Malvern PANalytical, reconstructing mineral profiles of the compounds by comparison with diffraction databases.

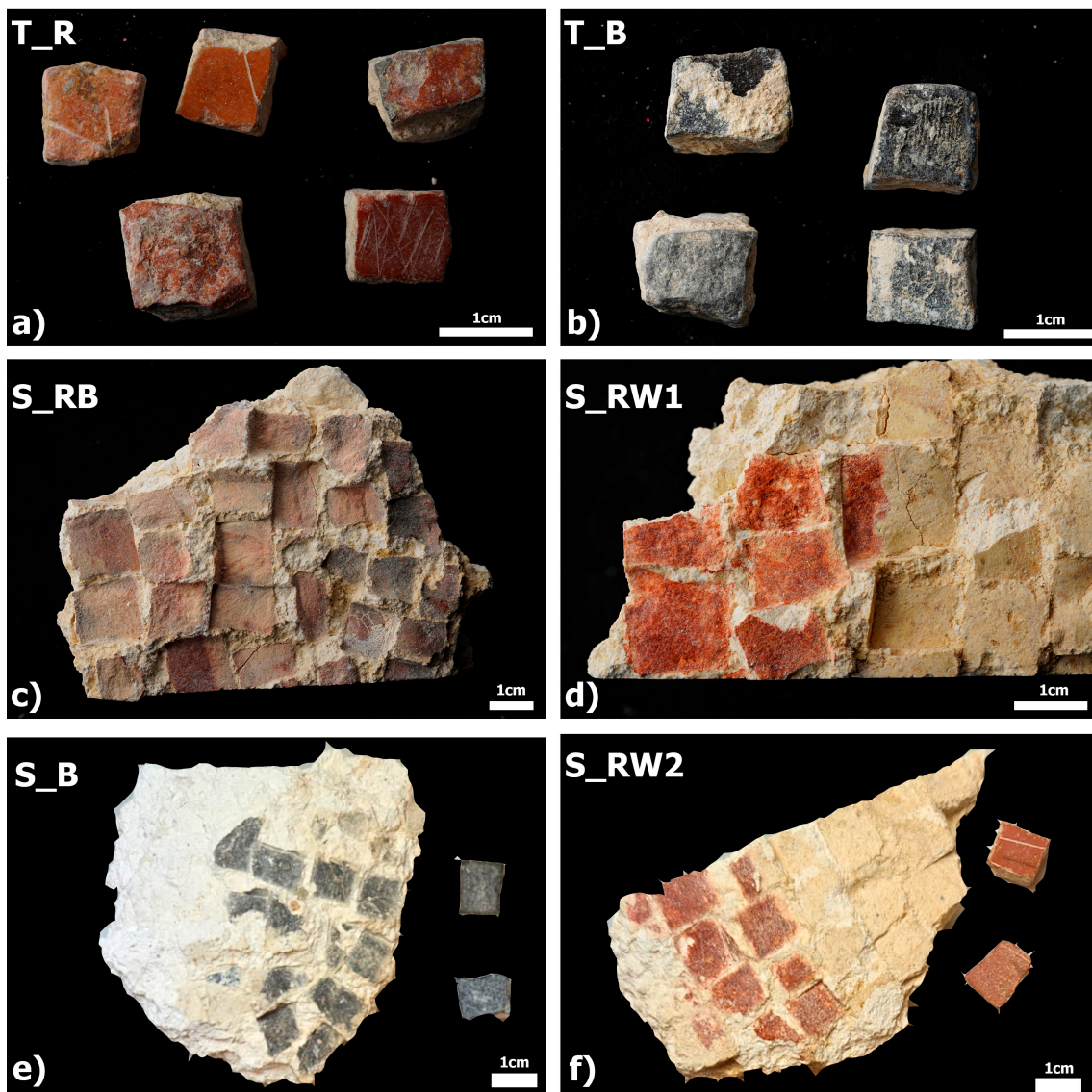


Figure 2. (a) Red (T_R) and (b) black (T_B) tesserae. (c) Red and black (S_RB) and (d) red and white (S_RW1) painted mortars (*sinopia*). (e) Black (S_B) and (f) red and white (S_RW2) painted mortars with their associated black and red tesserae that were removed manually.

Portable X-ray fluorescence spectrometry (pXRF) measurements were carried out on selected black and red painted sovrannucleus mortars (*sinopia*), the red and black tesserae, and unpainted rudus mortars below the painted areas. This was completed by placing a Bruker 5i Tracer handheld energy dispersive XRF spectrometer (Bruker Corporation, Billerica, MA, USA) on the area of interest. The diameter of the X-ray spot on the sample was approximately 7–8 mm and accurate positioning on the point to be analyzed was obtained by means of an integrated camera. The instrument was equipped with a Rh-anode, miniaturized X-ray tube operating at a maximum voltage of 50 kV, and with a Peltier-cooled high-resolution silicon drift detector (SDD). The semi-quantification of elements was provided by the instrument software, with a limit of detection of a few tens of ppm, based on built-in calibrations that were published elsewhere [23], averaging between 3 and 4 measurements for each sample.

Table 1. A list of the analyzed samples (tesserae and painted surfaces, i.e., *sinopia*) of the Birds Mosaic and relative analytical techniques used. Surface XRD measurements (no powders were prepared) were carried out on tesserae fresh cut (TF), top (S), and back (R) sides, and their locations mentioned in the sample notes. The apparent color is mentioned below the sample name.

	Sample Code	Notes	Sampling Required			Non-Invasive		
			TL-OM	SEM-EDS	FTIR	Surface-XRD	FORS	pXRF
Tesserae	T_B (black)	T_B(TF)	x	x		x		
		T_B(S)			x	x	x	x
		T_B(R)			x	x	x	x
	T_R (red)	T_R(TF)	x	x		x		
		T_R(S)			x	x	x	x
		T_R(R)			x	x	x	x
<i>Sinopia</i>	S_RB (red-black)	S_RB_1				x		
		S_RB_2				x		
		S_RB_A	x	x				
		S_RB_B	x	x				
	S_RW1 (red-white)	S_RW1_1				x		
		S_RW1_2				x	x	x
		S_RW1_C	x	x			x	x
	S_RW2 (red-white)	S_RW2_1			x		x	x
		S_RW2_2			x		x	x
	S_B (black)	S_B_1			x		x	x
S_B_2				x		x	x	

Fourier Transform Infrared spectroscopy (FTIR) analyses were carried using a Nicolet iS5 spectrometer (Thermo Fisher Scientific) on selected black and red painted sovranucleus mortars (*sinopia*), the red and black tesserae, and unpainted rudus mortars below the painted areas. Sampling was performed by carefully removing powder from the areas of interest using a scalpel, then crushing approximately 1 gr of sample by mortar and pestle for homogenization, and mixing approximately 50 mg with KBr. The mixture of KBr and sample was pressed in a PIKE handpress (PIKE Technologies, Madison, WI, USA) and measured once a clear pellet formed. Results, averaged from 32 scans at 4 cm⁻¹ resolution in the 400–4000 cm⁻¹ range, were analyzed in Omnic 8.3.

Fiber optic reflectance spectroscopy (FORS) measurements were carried out on painted surfaces using an ASD FieldSpec 4 Hi-Resolution Spectroradiometer (Malvern Panalytical) with a small diameter reflectance probe, which has a field spot of 1 mm. Each color on each fragment was tested at three locations. Results, averaged from 30 scans in the 400–2500 nm range, were analyzed in Omnic 8.3.

μ-Raman analyses were carried out using a Raman spectrometer (Renishaw inVia, Renishaw plc, Wotton-under-Edge, UK) equipped with a Leica DM LM optical microscope (Leica Microsystems, Wetzlar, Germany) and a high efficiency CCD detector. The measurements were performed in the spectral range of 100–1800 cm⁻¹ with a spectral resolution of 4 cm⁻¹. Microscope objective 20× was employed to focus the laser on the samples and to collect anelastic scattered radiations. The visual camera attached to the microscope allowed the selection of different points from which to collect Raman spectra, obtained by averaging 10 scans. A 785 nm excitation diode laser (HPNIR, Renishaw, 300 mW maximum laser power) with a grating of 1200 g/mm (gratings/mm) was used to analyze the black colored zones of the painted surfaces; whereas a 514 nm laser (Stellar-RMN, Modu-Laser, Centerville, UT, USA) with a maximum laser power below 48 mW and a

grating of 1800 g/mm (gratings/mm) was used for the inspection of red colored zones. Spectra manipulations and adjustments, such as smoothing and baseline subtraction, were performed using OriginPro9 software.

3. Results

Surface measurements using pXRF of the painted sovrannucleus (*sinopia*), unpainted rudus mortars, and associated tesserae show different compositions mainly in calcium, sulfur, and iron (Figure 3). Calcium is significantly higher in the tesserae (34–35%), indicating the material is composed of calcite and is presumably a carbonate rock, while the *sinopia* (14–17%) and the rudus mortars (21–24%) show that the lime was mixed with iron- and sulfur-based materials.

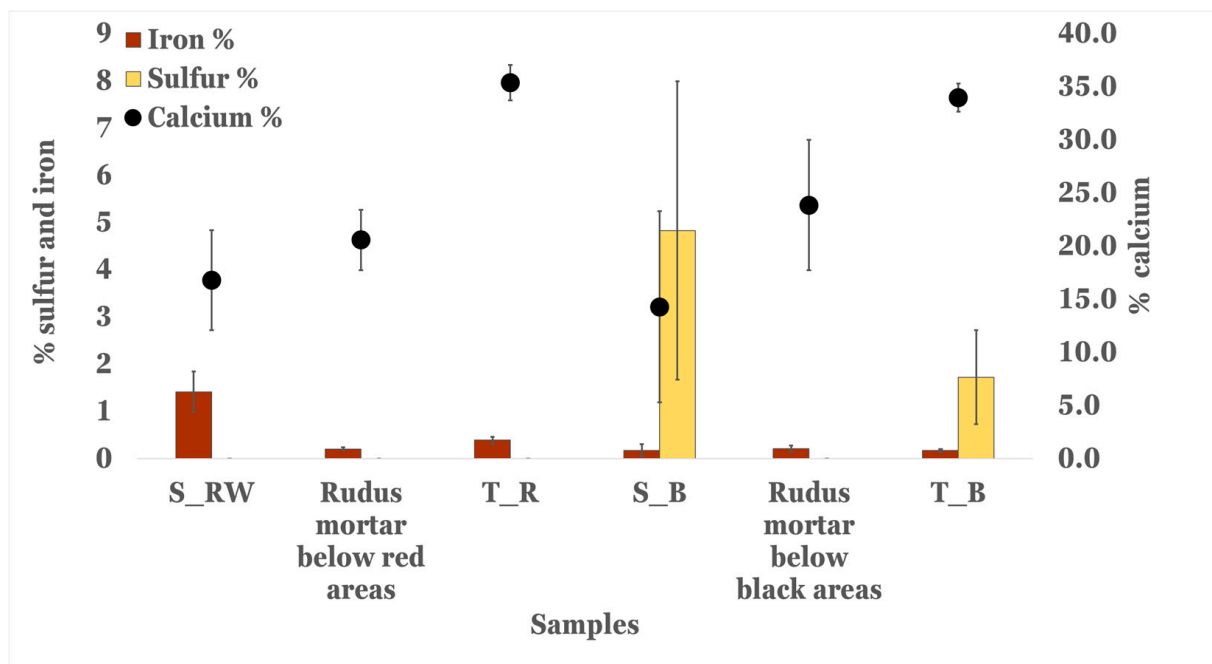


Figure 3. Non-invasive chemical analysis using a pXRF of painted sovrannucleus *sinopia* (S_RW and S_B), tesserae (T_R and T_B), and rudus mortars.

To understand the mineralogical composition of the materials, we applied FORS on the different surfaces, associating molecular structure to the elemental composition (Figure 4). The red materials in the *sinopia* and tesserae show broad absorption peaks at 1950 nm and 1450 nm, associated with clay's structural water combinations, and a prominent inflection at 575 nm, due to Fe^{3+} transition [24]. However, only the red painted areas show a large reflection peak at 740–750 nm, and a strong 860–890 nm absorbance peak (Laporte-forbidden transitions), which is associated with hematite (Fe_2O_3) in red ochre [25]. The broad reflection peak between 670 and 770 nm in the red tesserae, and the small absorption peak at 850 nm, suggest that the red colorants in the tesserae are materials with different molecular structures. This observation agrees with the higher iron values detected by the pXRF in the red painted areas. An additional prominent absorption peak at 2370 nm is observed, associated with the C-O bond of calcium carbonates with a slight shift to a higher wavelength due to the increased magnesium presence in the red tesserae [26]. The black materials in the *sinopia* and tesserae have smaller spectral features. We note that in the black *sinopia* there are sharper absorption peaks at 1450 nm, 1750 nm, and 1980 nm, associated with gypsum [27,28]. In the black tesserae we note absorption peaks at 2340 and 2370 nm, associated with the C-O bond of calcium carbonates, and 2205 nm from combination of O-H configurations. The presence of gypsum in the FORS spectra agrees with the higher sulfur values detected by the pXRF in the black painted areas.

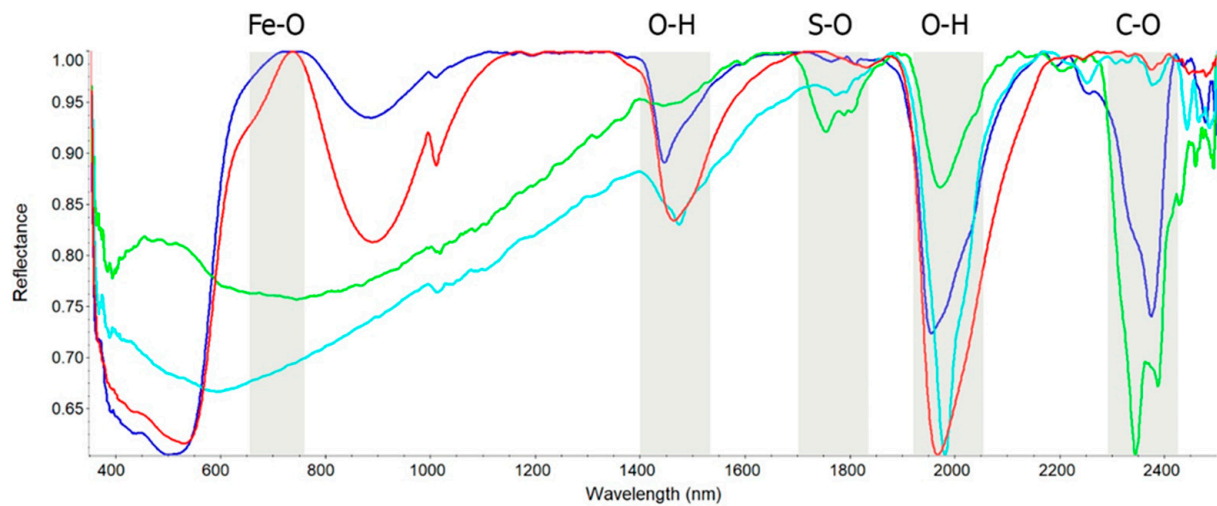


Figure 4. FORS spectra of black tesserae (green spectrum), black *sinopia* (turquoise), red tesserae (blue), and red *sinopia* (red). Labeled are the major vibrational bands of iron oxides (Fe-O), structural water in clays (O-H), sulfates (S-O), and carbonates (C-O).

The mineralogical compositions were verified by XRD, showing that the black and red tesserae are composed of calcite with a very low amount of quartz, dolomite, and halite (Table 2). In contrast, the supported painted surface mortar contains pigments, in particular the red areas (S_RB and S_RW1) show a high amount of hematite (up to 5%) with low quartz content. Halite was associated with secondary alteration processes in wall paintings [29]. The painted black and red areas in sample S_RB contain approximately 10% gypsum with low aliquots of quartz, hematite, and halite. This shows that hematite was used in the red mortar S_RW, and in the polychrome black and red mortar S_RB. The gypsum was only found in the black painted areas, and therefore we associate it with the use of the pigment (discussed below).

Table 2. A list of the relative percentages of mineralogical compositions of selected tesserae and *sinopia*. XRD measurements were carried on tesserae fresh cut (TF), top (S), and back (R) sides, noted in the sample notes, and the apparent color is mentioned below the sample name.

	Sample Code	Calcite	Dolomite	Gypsum	Quartz	Hematite	Halite	
Tesserae	T_B (black)	T_B(TF)	98	0	0	1	0	1
		T_B(S)	100	0	0	0	0	0
		T_B(R)	100	0	0	0	0	0
	T_R (red)	T_R(TF)	98	1	0	1	0	0
		T_R(S)	100	0	0	0	0	0
		T_R(R)	100	0	0	0	0	0
<i>Sinopia</i>	S_RB (red-black)	S_RB_1	85	0	11	1	3	1
		S_RB_2	91	0	7	1	1	1
	S_RW1 (red-white)	S_RW_1	71	0	0	1	2	25
		S_RW_2	75	0	0	1	5	19

To study the microstructure of the painted mortars and tesserae, a thin section analysis was performed. Petrographic analysis of the *sinopia* shows that the substrate mortar is based on a carbonate binder mixed with carbonate rock fragments (Figure 5). The painted *sinopia* is composed mainly of Ca-based materials, with different Fe-rich levels, based on EDS examinations. The red paint ranges between a 50 μm -thick layer (S_RB_B map 1) and a 100 μm -thick layer (map 2), indicating that the hematite was absorbed differently in the wet medium, in agreement with the fresco technique.

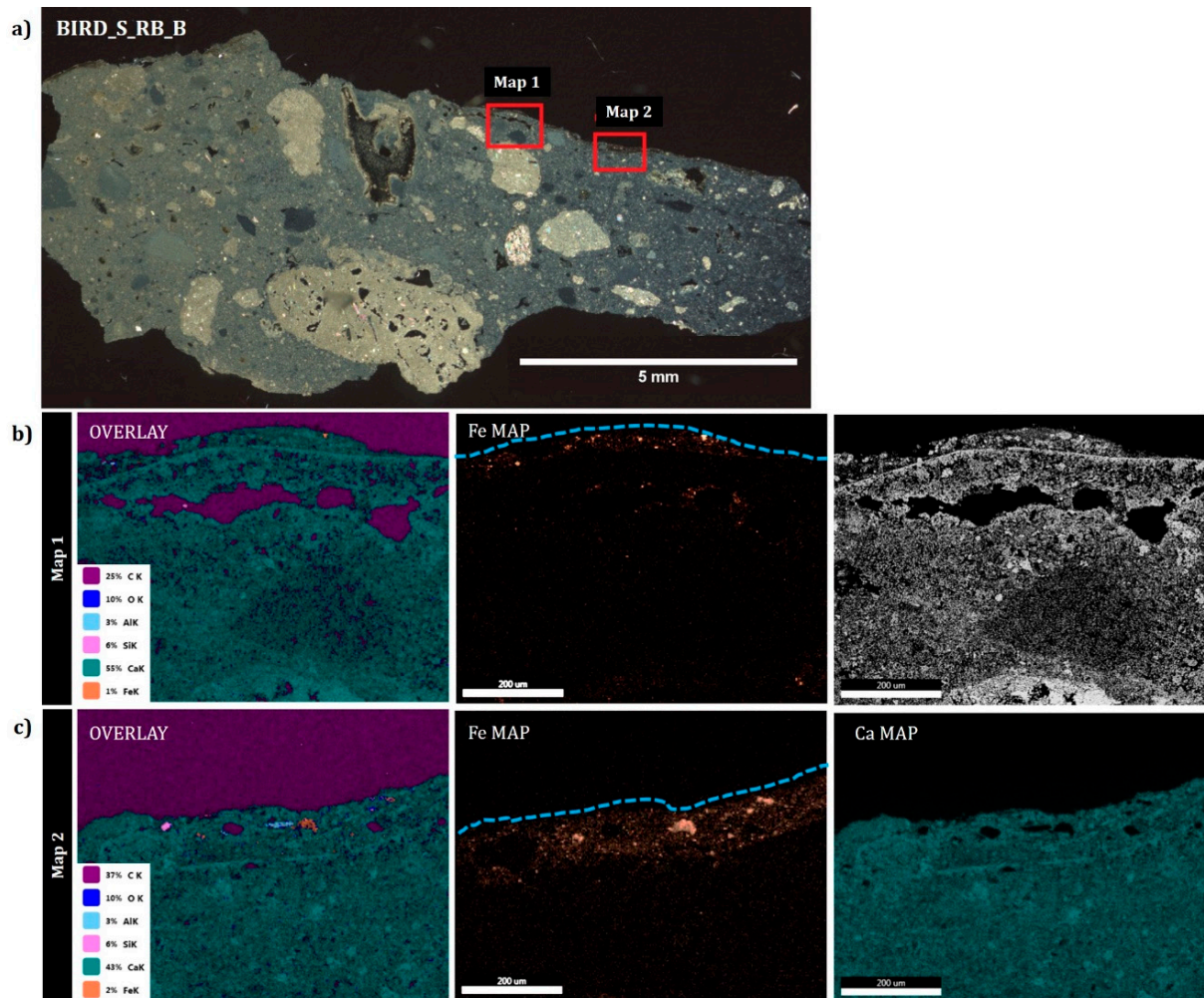


Figure 5. (a) Crossed polarized TL-OM micrographs of the thin cross section of the painted mortar (*sinopia*) sample S_RB_B with indication of the two elemental maps collected by ESEM-EDS analysis. (b) Map 1 and (c) Map 2 and elemental distribution and backscattered electrons images (BSI) of the two selected areas. The rim related to the sample surface has been highlighted by a blue dashed line.

The microstructure of the tesserae shows that the black tesserae contain biogenic nodules and a highly porous medium, based on petrographic and SEM images, while the red tesserae are homogenous and lack noteworthy features (Figure 6). The biogenic nodules in the black tesserae contain only calcium in EDS analysis, however, the matrix shows significant amounts of sulfur, which is associated with organic matter of degraded marine algae and phytoplankton [30].

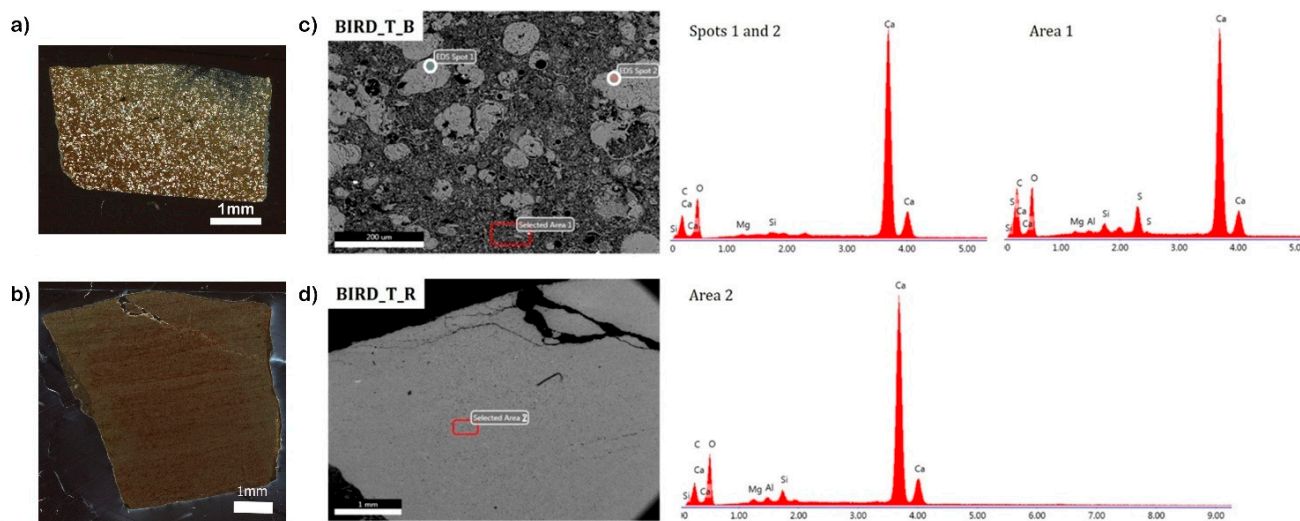


Figure 6. Mosaic tesserae thin sections analysis, showing crossed polarized TL-OM micrographs of the black (a) and red (b) stone tesserae, respectively. Backscattered electrons images (BSI) of the black (c) and red (d) stones, with indication of the spots and areas of EDS analyses reported alongside.

FTIR analysis of the tesserae, supporting mortar and painted mortars (*sinopia*), shows that they are based on calcite with different degrees of atomic disorder. Indeed, the different relative heights of the peaks at approximately 870 cm^{-1} (ν_2 , out-of-plane carbonate bending) and approximately 710 cm^{-1} (ν_4 , in-plane carbonate bending) in the IR spectra of calcite polymorphs have been related to atomic disorder in the lattice structure of calcium carbonate and can provide information on the type of calcium carbonate (plaster, chalk, and lime). Following Regev et al. [31], in Figure 7b, we plot the relative heights of ν_2 vs. ν_4 peaks in a graph with the expected trend lines for plaster, chalk, and lime. Results show the mortars are indeed highly disordered, indicating that they are well preserved. The tesserae have higher disorder values compared to limestone and chalk geological carbonates, suggesting that the rocks from which the tesserae were quarried underwent processes of diagenesis or heating. In addition, to understand the color in the black tesserae, they were dissolved, and the insoluble fraction was analyzed using FTIR. The spectra are similar to that of bitumen, containing vibrational bands of C-H organic compounds at 2852 and 2923 cm^{-1} , which could derive from degradation of biogenic products and be responsible to the black color of the stones. The black *sinopia* showed the presence of calcite and gypsum based on FTIR analysis of powders that were carefully removed from the surface. However, the underlying mortar below the black *sinopia* and the black tesserae showed only calcite. This indicates that the gypsum is only present in the painted black areas and did not migrate down into the porous lime mortar or up into the porous black stone. Similar observations were found in the red parts. The red *sinopia* contained hematite, while the mortar underlying the red *sinopia* and stones did not. Sodium nitrate, a soluble salt, was found in higher amounts in the red *sinopia* and its underlying lime mortar, and in smaller amounts in the black *sinopia* and its underlying lime mortar. This shows that soluble salts might have migrated between the layers, but gypsum, which is not as soluble, did not.

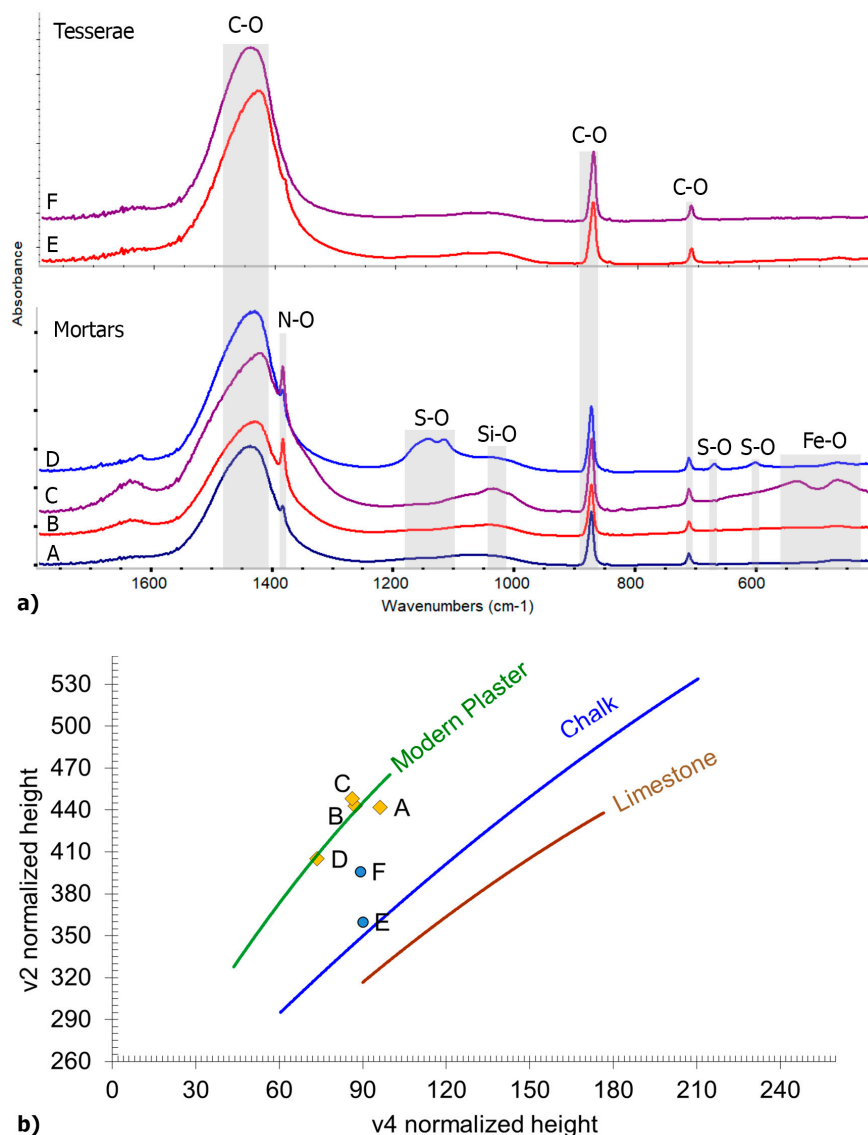


Figure 7. (a) FTIR spectra of the mortars and associated tesserae: rudas mortars below (A) black and (B) red areas, and painted sovrannucleus mortars (*sinopia*) with (C) red and (D) black pigments. Also shown are the (E) red and (F) black tesserae. Vibrational bands are labelled, associated with sodium nitrate (N-O), calcite (C-O), hematite (Fe-O), gypsum (S-O), and silicates (Si-O). (b) Internal atomic disorder of calcite in the mortars and tesserae, following Regev et al. [32] with labels matching the spectra.

Raman analysis of the red and black paints helped to understand the nature of the black pigment. Calcite and gypsum were detected by μ -Raman spectroscopy, based on their characteristic peaks at 265, 711, and 1082 cm^{-1} for the former, and 493 and 1007 cm^{-1} for the latter (Figure 8) [32]. Furthermore, the peaks located at ~ 1359 and 1597 cm^{-1} may correspond to the characteristic bands of the carbon black pigment that was previously found mixed with gypsum to heighten the black color of the pigment [33]. The Raman shift at 291, 416, and 606 cm^{-1} may be attributed to the bending and stretching modes of Fe-O in hematite [34,35], showing that it was used in the red paint (S_RW1) and the red and black paints (S_RB).

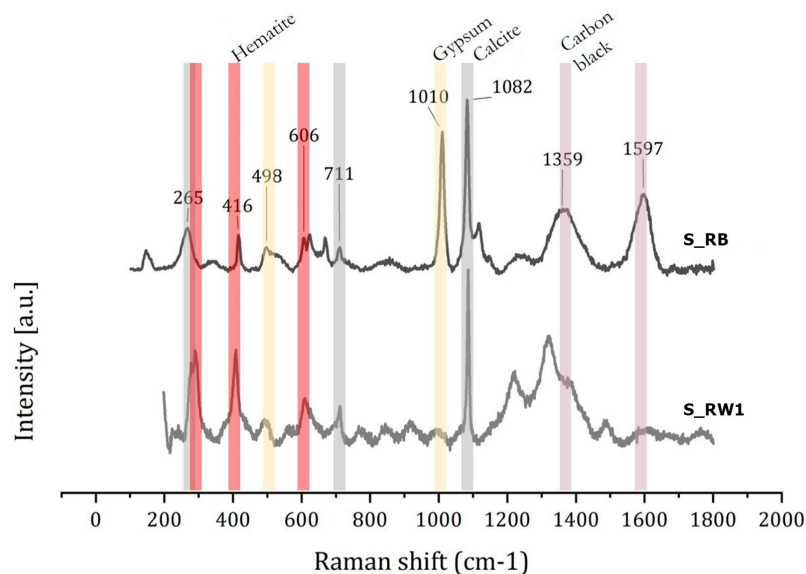


Figure 8. Representative μ -Raman spectra recorded in different points of the black (S_RB) and red (S_RW1) paints. The main peaks ascribable to the main minerals are highlighted.

4. Discussion

The stratigraphy of the Birds Mosaic follows the Vitruvian description, with two mortar layers between bedrock and tesserae, showing the lowest lime–mortar bed (rudus) is composed of lime mixed with millimeter-sized carbonate rocks and a low quantity of quartz. The upper fine mortar (sovrannucleus), where the mosaic tesserae were fixed, is based on micrometer-sized carbonate rock aggregates. Rectangular negatives are observed within the sovrannucleus, representing the locations where the tesserae were fixed. Some areas of the mortar were painted with red ochre and black carbon as indicators for the mosaicists to place the desired color of the stone following the content of the mosaic. Between the colored areas in the mortar, white mortar had risen, forming a 3D surface of the mortar, which indicates that the tesserae were fixed while the mortar was wet. To cover a large surface, such as the 27 m² of the Birds Mosaic, one can assume that the entire surface was not covered with a single layer of lime before the tesserae were fixed. This is because wet lime can dry rather quickly in the dry environment of the southern Levant, especially in the summer, which would risk the placement of the tesserae. This means that the painters, and the mosaicist who laid the stones, had to work on smaller parts of the mosaic, perhaps row by row or a few meters at a time, until the entire surface was complete.

Red paints in the mortar are characterized by larger quantities of hematite, as detected by XRD, FTIR, and Raman spectroscopy and confirmed by EDS elemental maps. The thickness of the Fe distribution in the sovrannucleus ranged between 50 and 100 μ m, and its homogenous dispersion supports the implementation of red ochre in the fresco technique. The black painted areas in the mixed red and black sample (S_RB) are characterized by low quantities of hematite, presumably from the adjacent red areas, and the presence of carbon black, as detected by μ -Raman spectroscopy. Interestingly, gypsum was also detected, but only in the black areas, and it was suggested that it heightens the black color [33]. This was a high level of sophistication and precision in material choices and execution, since it was found in the preparatory painting that was not meant to be revealed. These two pigments, hematite in red ochre and carbon black, individually or in combination, were both typically used for the *sinopia* in the Classic and Hellenistic periods [36]. These pigments were mostly used in *sinopiae* since they were accessible and cheap, compared to some exotic pigments such as cinnabar and Egyptian blue [37].

The analyzed mosaic tesserae (black and red) are both composed of a calcite-based matrix with no trace of hematite nor carbon black pigments, associating it with the local Mizzi Ahmar carbonate bedrock and Hatrurim formation, respectively. Local limestone,

known as Mizzi Ahmar, has been reported to have red bands, and is known to be quarried in the area of Jerusalem in antiquity [38]. Clay minerals such as illite and smectite may be related to the red colors of the limestone [39,40]. The SEM-EDS analysis of the red tesserae shows the presence of Mg, Al, and Si elements that could be correlated with the presence of clay minerals. Local black carbonate bedrock can be associated with the Hatrurim Formation [41], which is enriched in organic material; this conclusion is supported by the presence of sulfur and biogenic nodules in the black stone tesserae [30], and the presence of C-H organic compounds in FTIR vibrational bands.

The Byzantine Birds Mosaic can be compared to the Late Roman mosaic from Lod, since both show polychrome *sinopiae*, and stratigraphy that is similar to the one reported by Vitruvius [42]. Both mosaics show that the polychrome painted *sinopia* was applied with the fresco technique, with a high level of sophistication in pigments and painting techniques. However, the *sinopia* at Lod had a larger pigment palette and conserved features in the rudus mortar showed footprints of a sandal and bare feet. Footprints can say more about the weight and height, or age of people in the workshop [43].

Sinopiae are also interesting as they represent the original design, which sometimes changes [3]. In addition, these underlying contexts may preserve delicate features from chemical alterations and bioturbation, as a protected niche that preserves organic molecules and other information [40], since they are protected by the mosaic stone tesserae. Removal and relocation of mosaics as part of conservation efforts should take into account the information embedded in the multi-layered mortar structure below the tesserae. This study also provided insights into mosaic production techniques and the use of pigments, offering a unique glimpse into the ancient artistry and craftsmanship in mosaic workshops.

5. Conclusions

Mosaics are famous for the style and content represented by the tesserae upon which people walk. Their supporting surface is composed of mortar that is invisible to the crowd, with mainly functional properties. In this work, we studied the Armenian Chapel Birds Mosaic, which was constructed following a Vitruvian recipe. The painted mortar sketch found below the mosaic, known as a *sinopia*, was painted in the fresco technique with black carbon and red ochre pigments. These drawings were used as guidelines for the mosaicists in creating mosaics, facilitating the placement of colored tesserae in the supporting mortar. The tesserae were based on local red and black carbonate rocks, enriched in clays and organic material, respectively. This study also showed that mosaicists worked together with plaster painters at the executionary steps, when painting was followed by placing the tesserae, with implications for understanding ancient mosaic workshops.

Author Contributions: Conceptualization, Y.A., J.N., M.A. and G.A.; methodology, Y.A. and G.R.; software, A.L.; validation, Y.A. and G.R.; formal analysis, M.R., I.P. and A.L.; investigation, G.R., I.P. and A.L.; resources, Y.A. and G.A.; data curation, Y.A. and G.R.; writing—original draft preparation, Y.A. and G.R.; writing—review and editing, Y.A. and G.R.; visualization, Y.A. and G.R.; supervision, Y.A.; project administration, G.A. All authors have read and agreed to the published version of the manuscript.

Funding: This research received no external funding.

Data Availability Statement: The data presented in this study are available on request from the corresponding author due to the policy of the Israel Antiquities Authority.

Acknowledgments: We would like to thank Galeb Abu Diab for his input on the Armenian Birds Mosaic. We would like to thank the Lod Museum management for access to the materials in the museum, and Uzi 'Ad for his input and help.

Conflicts of Interest: The authors declare no conflicts of interest.

References

1. Arinat, M.; Shiyyab, A.; Al Sekhaneh, W. Analytical Characterization of Ancient Mosaic Floor Preparatory Layers and Tesserae from the Hippolytus Hall in Madaba, Jordan: Case Study. *Mediterr. Archaeol. Archaeom.* **2020**, *20*, 149–158.
2. Roncuzzi, I.; Fiorentini, E. *Mosaic: Materials, Techniques and History*; MweV: Lidcombe, Australia, 2002.
3. Hachlili, R. *Ancient Mosaic Pavements: Themes, Issues, and Trends Selected Studies*; Brill: Leiden, The Netherlands; Boston, MA, USA, 2009.
4. Cennini, C. *Il Libro dell'arte, o Trattato della Pittura di Cennino Cennini*; Le Monnier, F., Ed.; George Allen & Unwin, Ltd.: London, UK, 1859.
5. Dodge, B.K. *Tradition, Innovation, and Technique in Trecento Mural Painting: The Frescoes and Sinopie Attributed to Francesco Traini in the Camposanto in Pisa*; The Johns Hopkins University: Baltimore, MD, USA, 1978. (In Italian)
6. Murat, Z. Wall paintings through the ages: The medieval period (Italy, twelfth to fifteenth century). *Archaeol. Anthropol. Sci.* **2021**, *13*, 191. [[CrossRef](#)]
7. Salvadori, M.; Sbrolli, C. Wall paintings through the ages: The roman period—Republic and early Empire. *Archaeol. Anthropol. Sci.* **2021**, *13*, 187. [[CrossRef](#)]
8. Piovesan, R.; Maritan, L.; Neguer, J. The Polychrome Sinopia of Roman Mosaic at Lod (Israel): Pigments Characterization and Microstratigraphic Study. *Int. J. Herit. Digit. Era* **2012**, *1*, 203–208. [[CrossRef](#)]
9. Piovesan, R.; Mazzoli, C.; Maritan, L.; Cornale, P. Fresco and lime-paint: An experimental study and objective criteria for distinguishing between these painting techniques. *Archaeometry* **2012**, *54*, 723–736. [[CrossRef](#)]
10. Vitruvius. *The Ten Books of Architecture*; Morgan, M.H., Translator; Dover Publications Inc.: New York, NY, USA, 1960.
11. Storchan, B.; Asscher, Y. Provenance of Green Stone Tesserae from Byzantine Mosaics in the Judean Shephelah, Israel: Preliminary Results. *Archaeological Excavations and Research Studies in Southern Israel: Collected Papers Volume 5: 18th Annual Southern Conference 2022*. Available online: https://www.researchgate.net/publication/360219421_Provenance_of_Greenstone_Tesserae_from_Byzantine_Mosaics_in_the_Judean_Shephelah_Preliminary_Results#fullTextFileContent (accessed on 20 June 2024).
12. Licenziati, F.; Calligaro, T. Study of mosaic glass tesserae from Delos, Greece using a combination of portable μ -Raman and X-ray fluorescence spectrometry. *J. Archaeol. Sci. Rep.* **2016**, *7*, 640–648. [[CrossRef](#)]
13. Lysandrou, V.; Cerra, D.; Agapiou, A.; Charalambous, E.; Hadjimitsis, D.G. Towards a spectral library of Roman to Early Christian Cypriot floor mosaics. *J. Archaeol. Sci. Rep.* **2017**, *14*, 782–791. [[CrossRef](#)]
14. Re'em, A.; Abu Diab, G.; Neguer, J.; Nagar, Y.; Boaretto, E.; Tchekhanovets, Y. New Archaeological Study of the Armenian “Birds Mosaic” Chapel in Jerusalem. In *New Studies in the Archaeology of Jerusalem and Its Region*; Zelinger, Y., Peleg-Barkat, O., Uziel, J., Gadot, Y., Eds.; Israel Antiquities Authority: Jerusalem, Israel, 2021; Volume XIV: Collected Papers.
15. Gorzalczany, A.; Avissar, M.; Torgë, H.; 'Ad, U.; Jakoel, E.; Elisha, Y. Lod, the Lod Mosaic. *Hadashot Arkheologiyot: Excavations and Surveys in Israel*. 2016. Available online: http://www.hadashot-esi.org.il/report_detail_eng.aspx?id=24984 (accessed on 9 May 2016).
16. Piovesan, R.; Maritan, L.; Neguer, J. Characterising the unique polychrome sinopia under the Lod Mosaic, Israel: Pigments and painting technique. *J. Archaeol. Sci.* **2014**, *46*, 68–74. [[CrossRef](#)]
17. Murray, A.S. The Mosaic with Armenian Inscription from near the Damascus Gate, Jerusalem. *Palest. Explor. Q.* **1895**, *27*, 126–127. [[CrossRef](#)]
18. Von Schick, B.; Bliss, F.J. Discovery of a Beautiful Mosaic Pavement with Armenian Inscription, North of Jerusalem. *Palest. Explor. Q.* **1894**, *26*, 257–261. [[CrossRef](#)]
19. Stone, N. (Ed.) *Birds from Heaven in Heavenly Jerusalem*. In *Studies in Armenian Art: Collected Papers*; Armenian Texts and Studies; Brill: Leiden, The Netherlands; Boston, MA, USA, 2019; Volume 2, pp. 236–246.
20. Cotton, H.M.; Di Segni, L.; Eck, W.; Isaac, B.; Kushnir-Stein, A.; Misgav, H.; Price, J.; Yardeni, A. (Eds.) *Corpus Inscriptionum Iudaeae/Palaestinae*; De Gruyter: Berlin, Germany; Boston, MA, USA, 2012; Volume I: Jerusalem, Part 2, pp. 705–1120.
21. Avi-Yonah, M. Mosaic Pavements in Palestine. *Q. Dep. Antiq. Palest.* **1933**, *2*, 136–181.
22. Baraldi, P.; Bracci, S.; Cristoferi, E.; Fiorentino, S.; Vandini, M.; Venturi, E. Pigment characterization of drawings and painted layers under 5th–7th centuries wall mosaics from Ravenna (Italy). *J. Cult. Herit.* **2016**, *21*, 802–808. [[CrossRef](#)]
23. Rowe, H.; Hughes, N.; Robinson, K. The quantification and application of handheld energy-dispersive X-ray fluorescence (ED-XRF) in mudrock chemostratigraphy and geochemistry. *Chem. Geol.* **2012**, *324*, 122–131. [[CrossRef](#)]
24. Clark, R.N. *Spectroscopy of Rocks and Minerals, and Principles of Spectroscopy*; USGS: Reston, VA, USA, 2020.
25. Asscher, Y.; Angelini, I.; Secco, M.; Parisatto, M.; Chaban, A.; Deiana, R.; Artioli, G. Mineralogical interpretation of multispectral images: The case study of the pigments in the frigidarium of the Sarno Baths, Pompeii. *J. Archaeol. Sci. Rep.* **2021**, *35*, 102774. [[CrossRef](#)]
26. Hunt, G.R.; Salisbury, J.W.; Lenhoff, C.J. Visible and near-infrared spectra of minerals and rocks. VI. Sulfides and sulfates. *Mod. Geol.* **1971**, *3*, 1–14.
27. Cloutis, E.A.; Hawthorne, F.C.; Mertzman, S.A.; Krenn, K.; Craig, M.A.; Marcino, D.; Methot, M.; Strong, J.; Mustard, J.F.; Blaney, D.L.; et al. Detection and discrimination of sulfate minerals using reflectance spectroscopy. *Icarus* **2006**, *184*, 121–157. [[CrossRef](#)]
28. Crowley, J.K. Visible and Near-Infrared (0.4–2.5 μ m) Reflectance spectra of playa evaporite minerals. *J. Geophys. Res.* **1991**, *96*, 16231–16240. [[CrossRef](#)]

29. Angelini, I.; Asscher, Y.; Secco, M.; Parisatto, M.; Artioli, G. The pigments of the frigidarium in the Sarno Baths, Pompeii: Identification, stratigraphy and weathering. *J. Cult. Herit.* **2019**, *40*, 309–316. [[CrossRef](#)]
30. Sokol, E.V.; Kokh, S.N.; Sharygin, V.V.; Danilovsky, V.A.; Seryotkin, Y.V.; Liferovich, R.; Deviatiiarova, A.S.; Nigmatulina, E.N.; Karmanov, N.S. Mineralogical diversity of Ca₂SiO₄-bearing combustion metamorphic rocks in the Hatrurim Basin: Implications for storage and partitioning of elements in oil shale clinkering. *Minerals* **2019**, *9*, 465. [[CrossRef](#)]
31. Regev, L.; Poduska, K.M.; Addadi, L.; Weiner, S.; Boaretto, E. Distinguishing between calcites formed by different mechanisms using infrared spectrometry: Archaeological applications. *J. Archaeol. Sci.* **2010**, *37*, 3022–3029. [[CrossRef](#)]
32. Legodi, M.A.; de Waal, D. Raman spectroscopic study of ancient South African domestic clay pottery. *Spectrochim. Acta A Mol. Biomol. Spectrosc.* **2007**, *66*, 135–142. [[CrossRef](#)] [[PubMed](#)]
33. Hernanz, A.; Bratu, I.; Marutoiu, O.F.; Marutoiu, C.; Gavira-Vallejo, J.M.; Edwards, H.G.M. Micro-Raman spectroscopic investigation of external wall paintings from St. Dumitru’s Church, Suceava, Romania. *Anal. Bioanal. Chem.* **2008**, *392*, 263–268. [[CrossRef](#)]
34. Akyuz, S.; Akyuz, T.; Basaran, S.; Bolcal, C.; Gulec, A. Analysis of ancient potteries using FT-IR, micro-Raman and EDXRF spectrometry. *Vib. Spectrosc.* **2008**, *48*, 276–280. [[CrossRef](#)]
35. Ricci, G.; Caneve, L.; Pedron, D.; Holesch, N.; Zendri, E. A multi-spectroscopic study for the characterization and definition of production techniques of German ceramic sherds. *Microchem. J.* **2016**, *126*, 104–112. [[CrossRef](#)]
36. Eastaugh, N.; Walsh, V.; Chaplin, T.; Siddall, R. *Pigment Compendium*; Elsevier: Amsterdam, The Netherlands, 2008.
37. Becker, H. Outlining materiality: Color choice amongst preliminary drawings in roman painting. In Proceedings of the V Colloquio AIRPA—STRADE, Segni Tracce Disegni, Bologna, Italy, 13–15 June 2022; Associazione Italiana Ricerche Pittura Antica: Bologna, Italy, 2024, *in press*.
38. Avnimelech, M. Influence of geological conditions on the development of Jerusalem. *Bull. Am. Sch. Orient. Res.* **1966**, *181*, 24–31. [[CrossRef](#)]
39. Derrick, M.R.; Stulik, D.; Landry, J.M. *Scientific Tools for Conservation: Infrared Spectroscopy in Conservation Science*; The Getty Conservation Institute: Los Angeles, CA, USA, 1999; Volume 158.
40. Weiner, S. *Microarchaeology: Beyond the Visible Archaeological Record*; Cambridge University Press: Cambridge, UK, 2010.
41. Gross, S. *Petrographic Atlas of the Hatrurim Formation*; Geological Survey of Israel: Jerusalem, Israel, 2016.
42. Vitruvius. *Vitruvius: “Ten Books on Architecture”*; Cambridge University Press: Cambridge, UK, 2001.
43. Bennett, M.R. Prehistoric human footprint sites. In *Encyclopedia of Global Archaeology*; Springer International Publishing: Cham, Switzerland, 2020; pp. 8875–8879.

Disclaimer/Publisher’s Note: The statements, opinions and data contained in all publications are solely those of the individual author(s) and contributor(s) and not of MDPI and/or the editor(s). MDPI and/or the editor(s) disclaim responsibility for any injury to people or property resulting from any ideas, methods, instructions or products referred to in the content.